Available online at www.sciencedirect.com
SCIENCE DIRECT®
Theoretical Population Biology 67 (2005) 61–73
Theoretical Population Biology
www.elsevier.com/locate/ytpbi

Persistence, spread and the drift paradox

E. Pachepsky[a,*], F. Lutscher[b], R.M. Nisbet[a], M.A. Lewis[b,c]

[a]Department of Ecology, Evolution and Marine Biology, University of California Santa Barbara, Santa Barbara, CA 93106, USA
[b]Department of Mathematical and Statistical Sciences, University of Alberta, Edmonton, Alta., Canada T6G 2G1
[c]Department of Biological Sciences, University of Alberta, Edmonton, Alta., Canada T6G 2G1

Received 10 June 2003

Abstract

We derive conditions for persistence and spread of a population where individuals are either immobile or dispersing by advection and diffusion through a one-dimensional medium with a unidirectional flow. Reproduction occurs only in the stationary phase. Examples of such systems are found in rivers and streams, marine currents, and areas with prevalent wind direction. In streams, a long-standing question, dubbed 'the drift paradox', asks why aquatic insects faced with downstream drift are able to persist in upper stream reaches. For our two-phase model, persistence of the population is guaranteed if, at low population densities, the local growth rate of the stationary component of the population exceeds the rate of entry of individuals into the drift. Otherwise the persistence condition involves all the model parameters, and persistence requires a critical (minimum) domain size. We calculate the rate at which invasion fronts propagate up- and downstream, and show that persistence and ability to spread are closely connected: if the population cannot advance upstream against the flow, it also cannot persist on any finite spatial domain. By studying two limiting cases of our model, we show that residence in the immobile state always enhances population persistence. We use our findings to evaluate a number of mechanisms previously proposed in the ecological literature as resolutions of the drift paradox.

Keywords: Drift paradox; Stream; Aquatic insects; Propagation speed; Critical domain size; Persistence

1. Introduction

Many populations, communities, and ecosystems persist in environments where some or all life stages disperse in media with a strong directional bias. Examples include plants with windborn seeds, aquatic organisms in streams, rivers and estuaries, and marine organisms with larval dispersal influenced by ocean currents. One key issue for theory in stream ecology is the so-called ''drift paradox'', according to which extinction is inevitable in a closed population subject only to downstream drift. The analogous problem in coastal marine systems is population persistence and distribution in the presence of long-shore currents (e.g. Gaines and Bertness, 1992; Alexander and Roughgarden, 1996; Gaylord and Gaines, 2000). There are currently only a few theoretical papers to guide this work, notably Lewis et al. (1996), Ballyk et al. (1998), Ballyk and Smith (1999), and Speirs and Gurney (2001).

A variety of hypotheses involving some compensatory upstream movement have been proposed as resolutions of the drift paradox. The first hypothesis (Müller, 1954, 1982) is that adult insects balance out the downward drift of the insect larvae by flying upstream for oviposition. Another hypothesis was proposed by Waters (1972) who suggested that the paradox would be resolved if insects were to reside mainly on the benthos, and only the surplus over the local carrying capacity would drift downstream. Other movement mechanisms that could influence persistence in streams include refugia in streams (Lancaster and Hildrew, 1993a, b; Winterbottom et al., 1997a, b; Rempel et al., 1999; Lancaster, 2000), effect of variability in stream

*Corresponding author. Fax: +1 805 893 3777.
E-mail address: pachepsk@lifesci.ucsb.edu (E. Pachepsky).

0040-5809/$ - see front matter © 2004 Elsevier Inc. All rights reserved.
doi:10.1016/j.tpb.2004.09.001

flow direction (such as turbulence), insect swimming in the water column and crawling on the benthos (Anholt, 1995; Speirs and Gurney, 2001; Humphries and Ruxton, 2002). Experimental studies have focused on addressing the first hypothesis of compensatory adult flight, producing evidence both supporting (Waters, 1972; Hershey et al., 1993; Williams and Williams, 1993) and contrary to the hypothesis (Waters, 1972; Bird and Hynes, 1981; Winterbourn and Crowe, 2001). Adult flight patterns strongly depend on the species considered, and for species without an aerial stage this hypothesis is not applicable at all. There are experimental data for larval swimming and crawling on the benthos (Elliot, 1971; Waters, 1972; Poff and Ward, 1992; Humphries and Ruxton, 2002), but these experiments were not conducted specifically with the drift paradox in mind.

Modeling efforts have also addressed possible resolutions of the drift paradox. Anholt (1995), using a simulation model, concluded that, not only adult flight, but also any dispersal with upstream component could lead to population persistence. However, as pointed out by Speirs and Gurney (2001), he simulated a population with density dependence that strongly favored persistence. Ruxton and Humphries (2002) introduced some biological parameterization in Anholt's model, and showed that extinction may happen over a temporal scale so long that we may not be able to observe it. Speirs and Gurney (2001) concentrated on the role of diffusion, variability in river flow direction (e.g. due to tides), and swimming of organisms, as balancing mechanisms for the downstream drift. They offered quantitative predictions as to the balance between upstream diffusive movement and downstream flow necessary for persistence. Their simplest model was a simplified one-dimensional representation of a population residing in a stream, a river or an estuary subject to advection (stream flow) and diffusion (representing random movement):

$$\frac{\partial n}{\partial t} = f(n)n - v\frac{\partial n}{\partial x} + D\frac{\partial^2 n}{\partial x^2}. \tag{1}$$

Here, $n(x, t)$ is the density of the population per unit area, $f(n)$ is the local per capita growth rate of the population, v is the advection speed and D is the diffusion coefficient. No individuals enter at the top of the stream reach, and individuals in the stream cannot move beyond the top of the stream. This would occur if the top of the stream reach were the stream source, for example. At the bottom of the stream reach, individuals that cross the boundary never come back. An example of this would be a stream reach entering another stream. These zero-flux and hostile boundary conditions imply

$$vn(0,t) - D\left(\frac{\partial n}{\partial x}\right)_{x=0} = 0,\ n(L,t) = 0, \tag{2}$$

where $x = 0$ is the top, and $x = L$ is the end of the stream reach. Speirs and Gurney found the necessary balance between advection, critical domain size and the population growth rate necessary for persistence of a population described by (1). Using elaborations of their basic model, they explored effects of variability in advection speed on persistence and considered a stream reach with vertical variation in diffusivity. For each case they derived approximate requirements for population persistence.

In this work, we extend the model of Speirs and Gurney (2001) to address the issue of persistence of benthic aquatic organisms. For example, for some aquatic insects larvae reside mainly on the benthos, but move periodically by jumping into the flow and drifting downstream (Allan, 1995, pp. 221–229). Larvae stage lasts several months, and when adults emerge from the stream they live for a few days only. The model we consider can be used to explore the dynamics of a population of aquatic insect larvae without the effect of the adult movement. We divide the population into two interacting compartments: individuals residing on the benthos (the bottom of the stream) and individuals drifting in the flow. The importance of variable movement rates was demonstrated by Speirs and Gurney, when they considered variable diffusion through horizontal layers of the water column. Out extension is important because aquatic insect larvae spend a considerable proportion of their time immobile on the benthos. Moreover, the switching rates between benthos and drift may be set by insect behavior rather than by stream hydrodynamics. For example, there is evidence that the rate of entry into the drift can depend on the organisms response to environmental factors such as food abundance and density dependence (Hershey et al., 1993; Allan, 1995, pp. 229–237; Siler et al., 2001). The settling rate to the benthos has been shown experimentally to be roughly constant for some species (Elliot, 1971). In this paper, we assume that the rate of drift entry is constant, but the model we present is designed in a way that allows to easily incorporate these factors in future studies. Our model is similar to, but simpler than, the model analyzed by Ballyk and Smith (1999). They analyzed the dynamics of a bacterial population divided into wall-attached and unattached compartments competing for nutrient resource, and find possible steady states and conditions for their existence and stability.

Our results show that separating the population into two compartments has significant implications for population persistence. In particular, we calculate the critical domain size necessary for population persistence and estimate how much the compartmentalization of the population aids population persistence (see also Holmes, 2001). We also consider the ability of the population to spread up- and downstream and the speed at which this spread can occur. Our approach is closely

related to that used by Lewis and Schmitz (1996) who analyzed the propagation speed of a population with mobile and stationary compartments but without flow and with low rate of transfer from stationary to mobile compartments. We use and extend their results to the case with flow and no restrictions on the transfer rates. We also draw on work by Hadeler and Lewis (2004) who derive propagation speeds of a compartmentalized population without flow, but with mortality in the mobile compartment. The results include propagation speeds of a population spreading with and against the current as a function of stream flow.

We compare the propagation speeds of our model with the Speirs and Gurney (2001) model in order to evaluate the effect of compartmentalization on the propagation speed. Finally, we show that the persistence criteria and propagation speeds are closely related. This connection has not been explicitly brought out in the literature, as modeling efforts usually concentrate on one or the other feature. However, from a biological perspective the questions of persistence and invasion are clearly connected. We make this connection rigorously.

2. Model

Consider a population in which individuals live and reproduce on the benthos, and occasionally enter the water column to drift until they settle on the benthos again. Assume that (a) transfer between mobile to stationary compartments are via Poisson processes, (b) individual movement can be expressed as a combination of advection (corresponding to the uniform stream flow as experienced by the organisms) and diffusion (corresponding to the heterogeneous stream flow and individual swimming), (c) reproduction occurs on local scale, i.e. adult insects lay eggs where they emerge, yield the following system:

$$\begin{aligned}\frac{\partial n_d}{\partial t} &= \mu n_b - \sigma n_d - v\frac{\partial n_d}{\partial x} + D\frac{\partial^2 n_d}{\partial x^2},\\ \frac{\partial n_b}{\partial t} &= f(n_b)n_b - \mu n_b + \sigma n_d,\end{aligned} \tag{3}$$

where n_b is the population density on the benthos; n_d is the population density in the drift; $f(n_b)$ is the per capita rate of increase of the benthic population (we assume no Allee effect in the population, and thus the maximum per capita growth rate is found as the population density approaches zero, $f(0) = \max\{f(n_b)\}$); μ is the per capita rate at which individuals in the benthic population enter the drift; σ is the per capita rate at which the organisms return to benthic population from drifting; D is the diffusion coefficient; and v is the advection speed experienced by the organisms (we make a simplifying assumption that the stream advection is uniform in the horizontal and vertical directions). System (3) collapses into the single Fisher equation used in Speirs and Gurney (2001) in the two limiting situation which are discussed in Section 6.

3. Population persistence and critical domain size

In this section, we examine persistence criteria for a population described by (3). We assume the domain to be the one-dimensional interval $(0, L)$ representing a stream reach. For the drift population, we consider the same boundary conditions as Speirs and Gurney (2001), i.e. formula (2) above with n replaced by n_d. The ordinary differential equation for n_b does not require boundary conditions.

Since the maximum per capita growth rate is at low densities, population persistence is equivalent to population growth at small densities (Lewis and Kareiva, 1993). We therefore linearize system (3) around the zero steady state and obtain conditions under which a small population grows. The linearized system is the same as (3) with $f(n_b)$ replaced by $r = f'(0)$. We now rescale the system by setting

$$\tilde{t} = rt,\ \tilde{\mu} = \frac{\mu}{r},\ \tilde{\sigma} = \frac{\sigma}{r},\ \tilde{x} = \frac{x}{\sqrt{D/r}} \text{ and } \tilde{v} = \frac{v}{\sqrt{Dr}}.$$

We drop the tildes for convenience, so that system (3) becomes

$$\begin{aligned}\frac{\partial n_d}{\partial t} &= \mu n_b - \sigma n_d - v\frac{\partial n_d}{\partial x} + \frac{\partial^2 n_d}{\partial x^2},\\ \frac{\partial n_b}{\partial t} &= (1-\mu)n_b + \sigma n_d.\end{aligned} \tag{4}$$

We consider the two cases $\mu < 1$ and $\mu \geqslant 1$ separately.

3.1. Case 1: $\mu < 1$

In this case, the rate at which individuals leave the benthos is smaller than the local growth rate, and therefore the net growth rate of the benthic population at each spatial location is positive. Under these conditions, persistence is guaranteed irrespective of the domain length and the advection speed. To see this, consider the dynamics of the benthic population, n_b (second equation in (4)):

$$\frac{\partial n_b}{\partial t} = (1-\mu)n_b + \sigma n_d \geqslant (1-\mu)n_b,$$

since n_d is non-negative for non-negative initial values according to the maximum principle (Strauss, 1992). Hence, the population on the benthos grows at least exponentially when population levels are small, and so the population persists.

3.2. Case 2: $\mu \geqslant 1$

If $\mu > 1$, the leaving rate of the benthic population into the drift is higher than the local growth rate. We show that persistence is possible provided that the domain L is large enough with respect to the advection speed v (see also Hadeler and Lewis, 2004). In Appendix A, we derive the condition for population persistence to be

$$\lambda_1 < \frac{\sigma}{\mu - 1}, \tag{5}$$

where λ_1 is the smallest real solution to

$$\frac{\sqrt{4\lambda_n - v^2}}{v} + \tan\left(\frac{\sqrt{4\lambda_n - v^2}}{2} L\right) = 0. \tag{6}$$

From this we can establish the relationship between L and v to be

$$L = \frac{2}{\sqrt{\frac{4\sigma}{\mu-1} - v^2}} \tan^{-1}\left(-\frac{1}{v}\sqrt{\frac{4\sigma}{\mu - 1} - v^2}\right). \tag{7}$$

If L is greater than the expression on the right, the population can persist, if L is smaller, then the population will go extinct, see Fig. 1. The critical domain size increases as advection increases. This is consistent with the intuition that with faster advection, a population will require a larger domain size to persist. Fig. 1 also shows that the critical domain size tends to infinity for a threshold value of v_L^*, above which the population cannot persist on a domain of any size. This threshold value can be computed from (7). Since $\tan^{-1}$ is bounded, L tends to infinity for

$$v \to v_L^* = 2\sqrt{\frac{\sigma}{\mu - 1}}. \tag{8}$$

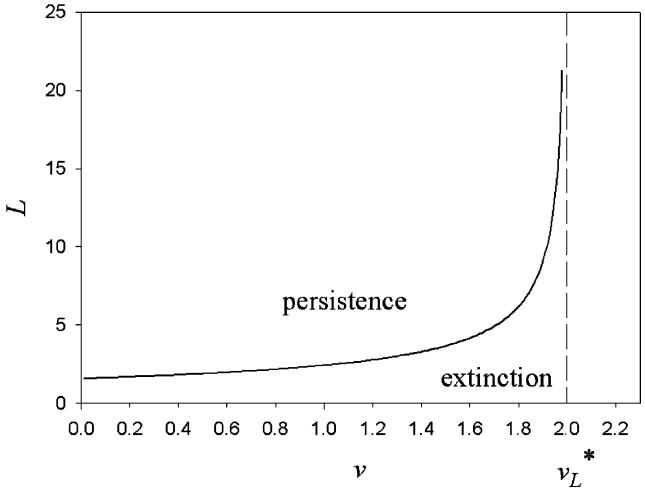

Fig. 1. The critical domains length L for a given value of advection v. Parameter values used are $\mu = 1.8$ and $\sigma = 0.8$, but the shape holds for all values of $\mu > 1$ that were investigated.

Finally, as $\mu \to 1$, condition (5) is always satisfied and the threshold value v_L^* tends to infinity, so that the population always persists, just as in Section 3.1 above.

4. Propagation speed

In the previous section, we derived conditions for population persistence of a system described by (3). In this section, we consider spatial spread of the population in time. For Fisher's equation without advection, a population forms traveling waves that spread through the domain with speed $c^* = 2\sqrt{Dr}$, where D is the diffusion coefficient and r is the intrinsic growth rate of the population (Murray, 1989). When we introduce advection into the system, we need to distinguish between the propagation speed downstream (in the direction of advection) and upstream (against the advection). With increasing advection, the propagation speed downstream increases, whereas the propagation speed upstream decreases. By changing to moving

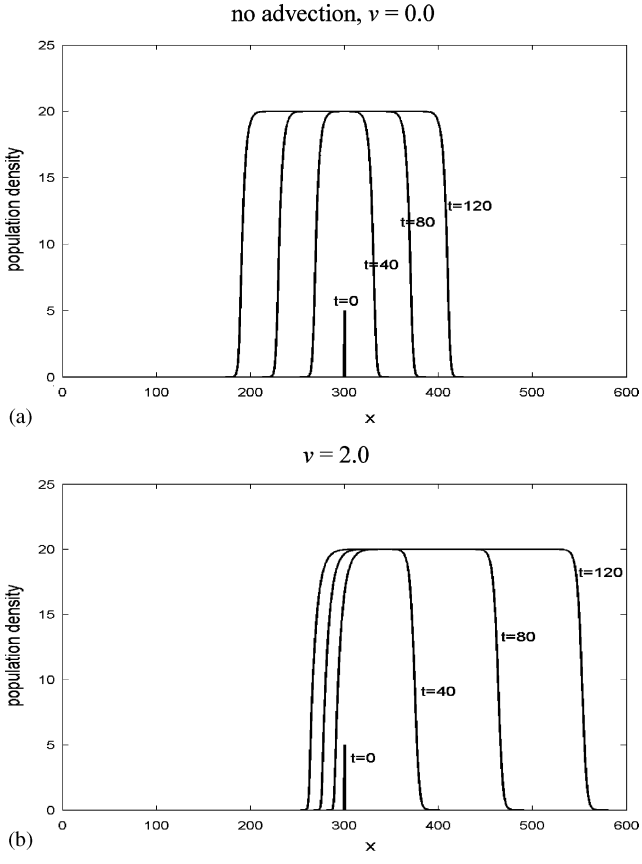

Fig. 2. Numerical simulation of a population invading a region in the case $\mu < 1 : \mu = 0.8$, $\sigma = 0.8$. The population consists of two compartments: individuals on the benthos and in the drift. The plots show the total of these two at different times t. The movement of the population occurs through diffusion and advection of the drifting individuals.

coordinates, it can be shown that the propagation speed downstream for a system described by a Fisher's equation with advection $v>0$ is (c^*+v) and the propagation speed upstream is (c^*-v). The resulting traveling waves are similar to the ones in Fig. 2 which shows a simulation of the system considered in this paper.

We now determine the up- and downstream propagation speeds for our system (3) representing a population with benthic and drift components. We assume that the benthic population has non-linear density dependence described by logistic growth. We use analytical and numerical methods to determine the propagation speed of traveling waves in this population. As in the previous analysis of persistence, we have to consider two cases. If the intrinsic growth rate is greater than the rate at which individuals change into the drift, then we know from the results in the previous section that the population will persist. Hence, we expect the population to spread upstream *and* downstream. Fig. 2 shows a numerical simulation of this situation (a) without and (b) with advection. Even in the presence of advection, the population does spread in both directions, but compared to the case without advection, the population spreads downstream faster and upstream slower. In the case when the intrinsic growth rate is less than the rate at which individuals switch into the drift, we expect that for large enough advection speeds, the population cannot persist and is washed out. The numerical simulations in Fig. 3 show the three possible outcomes. Without advection, the population spreads symmetrically as before (Fig. 3a); for small v, the population spreads in both directions with a bias downstream (Fig. 3b); and for large v, the population is washed downstream (Fig. 3c).

Mathematically, it is convenient to consider a situation where a population invades an uninhabited terrain as depicted in Fig. 4. In simulations, the population spreads in a large finite domain, but the mathematical analysis assumes a limiting case when the domain becomes infinite. We analytically determine the propagation speeds using the mathematical analysis, and then confirm that our analytical results match the numerical simulations.

To determine the up- and downstream propagation speeds, we first recast the system in traveling wave coordinates, then transform it into a system of first-order equations. We then can linearize it around the zero and the non-zero steady states, which informs us about the stability of the manifolds around the steady states. The requirements for stability lead to conditions, which allow us to determine the propagation speeds.

We consider a system (3) with logistic growth with carrying capacity K and intrinsic growth rate r. Retaining our previous scaling, in addition setting $\tilde{n}_d = \frac{n_d}{K}$ and $\tilde{n}_b = \frac{n_b}{K}$, and dropping the tildes for convenience,

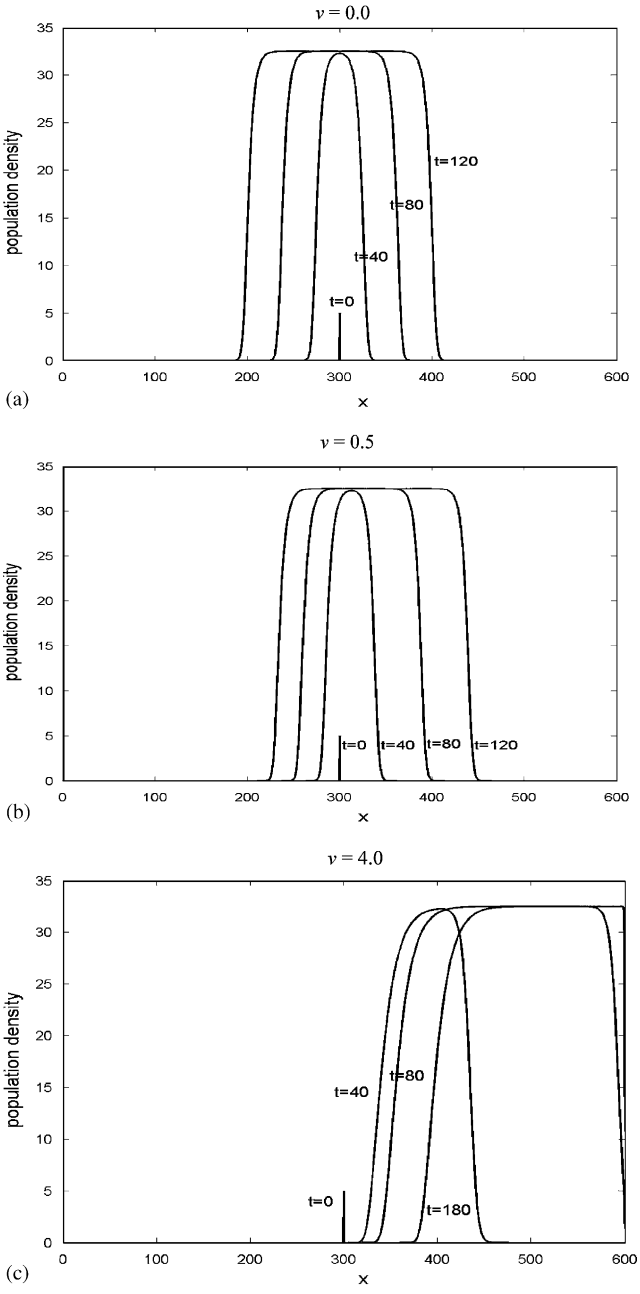

Fig. 3. Example of numerical simulations of the system in the case $\mu \geqslant 1$. Here shown for $\mu = 1.8$ and $\sigma = 0.8$. The plots show the total density of benthic and drifting individuals at different times t.

we obtain

$$\begin{aligned} \frac{\partial n_d}{\partial t} &= \mu n_b - \sigma n_d - v\frac{\partial n_d}{\partial x} + \frac{\partial^2 n_d}{\partial x^2}, \\ \frac{\partial n_b}{\partial t} &= n_b(1-n_b) - \mu n_b + \sigma n_d. \end{aligned} \tag{9}$$

The spatially homogeneous solutions to (9) are the zero steady state $(n_b, n_d) = (0,0)$ and the non-zero steady state $(n_b^*, n_d^*) = (1, \frac{\mu}{\sigma})$. We assume that there is a traveling wave connecting the non-zero to the zero steady state, i.e. there are solutions of (9) of the form

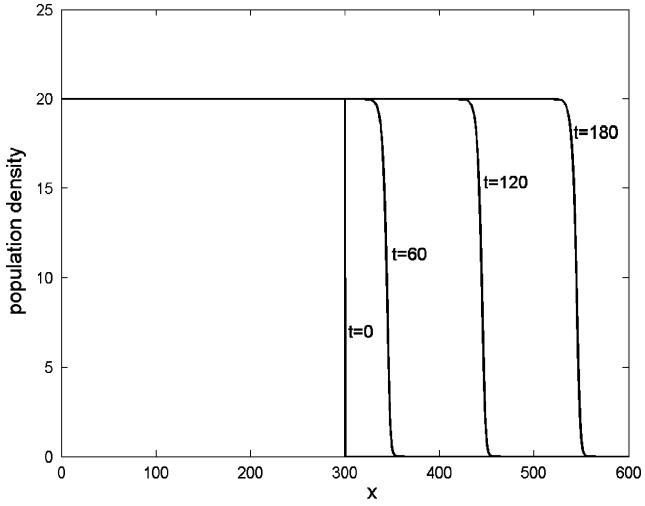

Fig. 4. Numerical simulations that can be represented mathematically. Initially, a population occupies the domain on $x \in [0, 300]$. The simulation shows a population spreading into an uninhabited domain on $x \in (300, 600]$. Here, if $v>0$ the population is spreading downstream, and if $v<0$ the population is spreading upstream. In this simulation $v = 0.5$, and $c>0$ (that is, population is spreading). A washout, corresponding to $c<0$, would occur if v is large and negative.

$(n_b, n_d)(x, t) = (N_b, N_d)(x - ct) = (N_b, N_d)(z)$. Here, c is the wave propagation speed.

We can rewrite (9) as

$$\begin{aligned} -cN_d' &= \mu N_b - \sigma N_d - vN_d' + N_d'', \\ -cN_b' &= N_b(1 - N_b) - \mu N_b + \sigma N_d, \end{aligned} \tag{10}$$

where the prime denotes differentiation with respect to z. In the presence of advection, we need to consider two types of waves, downstream facing waves and upstream facing waves. For a downstream facing wave, the asymptotic boundary conditions for N_b, N_d, and $M = N_d'$ are

$$\begin{aligned} &N_b(-\infty) = 1,\ N_d(-\infty) = \tfrac{\mu}{\sigma},\ M(-\infty) = 0, \\ &\quad N_b(\infty) = 0,\ N_d(\infty) = 0,\ M(\infty) = 0. \end{aligned} \tag{11}$$

These represent a wave as plotted in Fig. 4. An upstream facing wave has asymptotic boundary conditions

$$\begin{aligned} &N_b(-\infty) = 0,\ N_d(-\infty) = 0,\ M(-\infty) = 0, \\ &\quad N_b(\infty) = 1,\ N_d(\infty) = \tfrac{\mu}{\sigma},\ M(\infty) = 0. \end{aligned} \tag{12}$$

Note that in this case if c is positive, the population is retreating with the flow; if c is negative, the population is spreading upstream.

System (10) is equivalent to the following system of three differential equations:

$$\begin{aligned} N_d' &= M, \\ M' &= -\mu N_b + \sigma N_d - (c - v)M, \\ N_b' &= \frac{N_b^2}{c} - \frac{(1-\mu)N_b}{c} - \frac{\sigma}{c}N_d. \end{aligned} \tag{13}$$

We now linearize (13) around the zero and the non-zero steady states, and the real parts of the eigenvalues of the characteristic polynomials determine the dimension of the stable and unstable manifolds.

Linearization of (13) around the zero steady state yields the characteristic polynomial

$$P_0(\lambda) = -\lambda^3 + A_1\lambda^2 + A_2\lambda + A_3 = 0, \tag{14}$$

where

$$\begin{aligned} A_1 &= \frac{\mu - 1}{c} - (c - v), \\ A_2 &= (\mu - 1)\left(1 - \frac{v}{c}\right) + \sigma, \\ A_3 &= \frac{\sigma}{c}. \end{aligned} \tag{15}$$

If at least one of the roots of P_0 is negative, then the dimension of the stable manifold is one or more.

Linearizing (13) around the non-zero steady state yields the characteristic polynomial

$$P_1(\lambda) = -\lambda^3 + B_1\lambda^2 + B_2\lambda + B_3 = 0, \tag{16}$$

where

$$\begin{aligned} B_1 &= \frac{\mu + 1}{c} - (c - v), \\ B_2 &= (\mu + 1)\left(1 - \frac{v}{c}\right) + \sigma, \\ B_3 &= \frac{\sigma}{c}. \end{aligned} \tag{17}$$

If at least one of the roots of P_1 is positive, then the dimension of the unstable manifold is one or more.

We consider three cases $\mu<1$, $\mu = 1$ and $\mu>1$. In the previous section, we showed that, for the first two, persistence is guaranteed, and for the last one washout is possible. If $\mu<1$, we conclude that the population will always spread both up- and downstream. This can be shown using the argument from Lewis and Schmitz (1996), which holds for our system.

In Appendix B we show the derivation of the up- and downstream propagation speed c^* of the traveling waves. Fig. 5 shows a plot of the propagation speed c^* as a function of the advection speed v as predicted by the analysis. The downstream propagation speed increases with advection speed, while the upstream propagation speed decreases with advection speed, but remains positive. Fig. 5 also shows the propagation speeds for two values of v obtained from simulations in Fig. 2. The propagation speeds obtained from simulations agree with the propagation speeds obtained analytically.

If $\mu \geqslant 1$, when rate of transfer into the drift exceeds the intrinsic growth rate, the upstream propagation speed need no longer remain positive. On the contrary, we expect that for large values of v, the population will be washed down the domain (as in Fig. 3c). In Appendix B, we show the derivation of the up- and downstream propagation speed c^* of the traveling waves. If $\mu = 1$

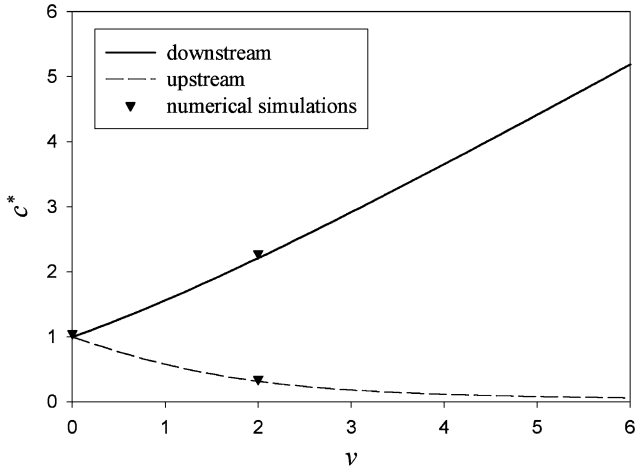

Fig. 5. Propagation speeds upstream and downstream as a function of the advection velocity v. Case $\mu<1$, here shown for $\mu=0.8$ and $\sigma=0.8$. Propagation speeds upstream never become negative, i.e. the population is never washed downstream.

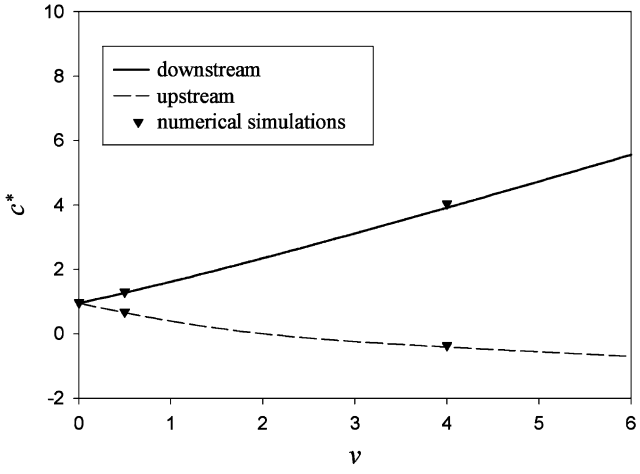

Fig. 6. Propagation speeds in case when $\mu\geqslant 1$. Shown for $\mu=1.8$ and $\sigma=0.8$. The upstream propagation speed becomes negative at a critical value v_c^*.

then the propagation speeds up- and downstream are always positive, as for the case $\mu<1$. If $\mu>1$, then washout is possible. Fig. 6 shows the propagation speeds up- and downstream as a function of the advection speed v, along with the values of propagation speeds obtained numerically from simulations in Fig. 3. The downstream propagation speed increases with increasing advection. The upstream propagation speed decreases with increasing advection and, at a critical value v_c^*, switches from positive to negative. The critical value v_c^* can be calculated as follows. Multiplying the Eq. (14) by c we obtain

$$-c\lambda^3+((\mu-1)-c(c-v))\lambda^2 +((\mu-1)(c-v)+cv)\lambda+\sigma=0. \tag{18}$$

For $c\to 0$ this becomes

$$(\mu-1)\lambda^2-(\mu-1)v_c^*\lambda+\sigma=0. \tag{19}$$

This has a zero of multiplicity 2 if and only if

$$v_c^*=2\sqrt{\frac{\sigma}{\mu-1}}. \tag{20}$$

5. Connection between the propagation speed and the critical domain size

From a biological perspective, persistence and ability to propagate should be closely connected. If a population cannot propagate upstream but is washed downstream, it will not persist. However, this connection has not previously been explicitly addressed in a mathematical framework. In this section, we draw on the connection between the analytical results for the Fisher's equation with advection (1) and the stream system (3). One of the results of Speirs and Gurney (2001) for the Fisher's equation with advection is that persistence is possible in a population if

$$v<2\sqrt{Dr}. \tag{21}$$

Note that $c^*=2\sqrt{Dr}$ is the propagation speed of a traveling wave in a Fisher's equation without advection. In fact, as mentioned in the previous section, the propagation speed upstream of a traveling wave in Fisher's equation is (c^*-v). Therefore, the conclusion of Speirs and Gurney in (23) is equivalent to saying that the upstream propagation speed must be positive. If it is negative, the population is washed downstream and therefore cannot persist.

We now address the same question in system (3) with the benthic and drift components. Comparing Eqs. (8) and (20) we can see that the advection speed $v_{L,}^*$ for which the upstream speed switches from positive to negative, is equal to v_c^* the advection speed for which the critical domain size approaches infinity. That is, the upper limit of the advection that allows a population to persist on a finite domain is the same as the threshold advection speed when the wave switches from propagating up the stream to retreating down the stream. Fig. 7 shows the relationship between the propagation speed and the critical domain size.

6. Effect of the stationary component on population persistence and spread

We now show the effect of separating of the population into mobile and stationary compartments on persistence. To do this, we compare dynamics of the equation with stationary and mobile compartments to dynamics of two approximations in which the

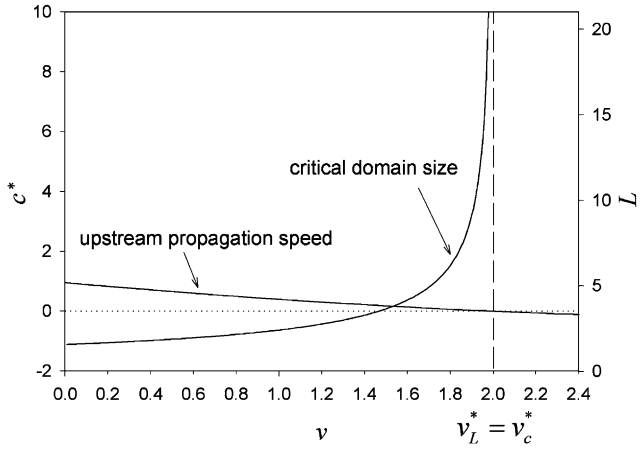

Fig. 7. The plot shows the critical domain size (right axis) and the upstream propagation speed (left axis) on the same plot as a function of the advection speed v. v_L^* is the advection speed for which the critical domain size becomes infinite is equal to v_c^* for which the propagation speed upstream switches between positive and negative. Shown for $\mu = 1.8$ and $\sigma = 0.8$.

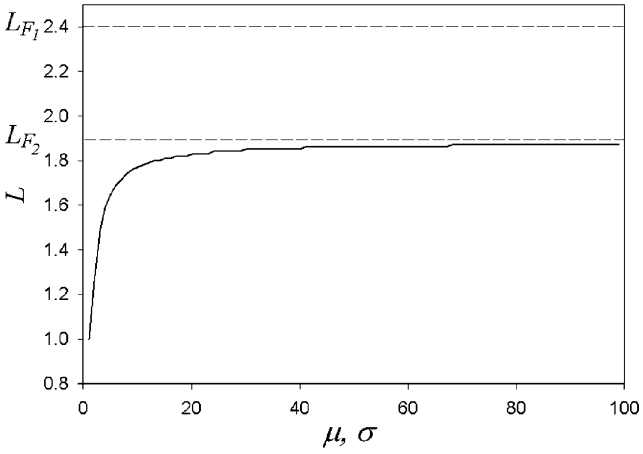

Fig. 8. Critical domain size as a function of μ and σ for $v = 0.5$. A point x on the x-axis corresponds to the case $\mu = \sigma = x$. The critical domain size approaches $L_{F2} \approx 1.88$, the critical domain size in the second Fisher approximation. The first Fisher approximation gives a bigger critical domain length $L_{F1} \approx 2.42$.

compartments are combined. First, we can ignore that individuals are stationary for a part of their lifetime and combine the two equations of (3) into a single Fisher's equation and modeled by (1). We refer to this as the first Fisher approximation. We can also consider a limiting case of system (3) when the exchange between the benthic and drift components of the population occurs on a fast timescale (σ, $\mu \to \infty$ with $\sigma = \tau\mu$). Since $\mu \to \infty$, the second equation in (3) yields $n_b = \tau n_d$. Summing the first and the second equations of (3) we obtain

$$\frac{\partial n_b}{\partial t} = \tilde{f}(n_b)n_b + \tilde{D}\frac{\partial^2 n_b}{\partial x^2} - \tilde{v}\frac{\partial n_b}{\partial x}, \tag{22}$$

which is of the same form as (1), with

$$\tilde{f}(n_b) = \frac{f(n_b)}{(1+1/\tau)},\ \tilde{D} = \frac{D}{\tau+1} \text{ and } \tilde{v} = \frac{v}{\tau+1}, \tag{23}$$

where $f(n_b)$, D and v are the parameters of (3). For simplicity, we set $\tau = 1$, but the results presented below are independent of the value of τ. We refer to this as the second Fisher approximation.

We now examine how close the critical domain size and propagation speed of (3) are to the speed of two Fisher approximations. Fig. 8 shows the critical domain size of the system (3) as a function of μ and σ for $v = 0.5$. It also shows the critical domain size for the two Fisher approximations. For the first approximation the critical domain size is $L_{F1} \approx 2.42$. The critical domain size for the second Fisher approximation, $L_{F2} \approx 1.88$, is lower. For a Fisher equation with parameters, D, r and v, the critical domain size is given by

$$\frac{L_F}{L_d} = \left[\sqrt{\frac{v_d^2}{v_d^2 - v^2}}\right] \arctan\left[-\sqrt{\frac{v_d^2 - v^2}{v^2}}\right], \tag{24}$$

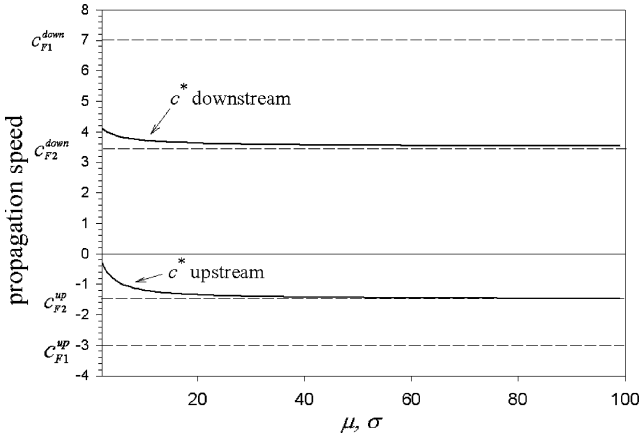

Fig. 9. Up- and downstream propagation speeds as a function of μ and σ for $v = 5.0$. A point x on the x-axis corresponds to the case $\mu = \sigma = x$. The dashed lines correspond to the two Fisher equation approximation: c_{F1}^{down} and c_{F1}^{up} correspond to down- and upstream speeds respectively of the first Fisher approximation; and c_{F2}^{down} and c_{F2}^{up} correspond to down- and upstream speeds, respectively, of the second Fisher approximation.

where $L_d = \sqrt{D/r}$ and $v_d = 2\sqrt{Dr}$, and $r = f'(0)$, see Speirs and Gurney (2001). The critical domain size approaches the smaller critical domain size L_{F2} from below as μ and σ become large. Fig. 8 shows that system with two components requires a smaller critical domain size than either of the limiting cases considered. This means that finite residence time on the benthos (μ, $\sigma < \infty$) enhances persistence of a population.

Fig. 9 shows the upstream and downstream propagation speeds vs. μ and σ under the assumption of logistic growth. It also shows the propagation speed predicted by two Fisher equation approximations: (a) downstream $c_{F1}^{down} = (2\sqrt{rD} + v)$ and upstream $c_{F1}^{up} = (2\sqrt{rD} - v)$; and (b) downstream $c_{F2}^{down} = (2\sqrt{\tilde{r}\tilde{D}} + v)$ and upstream

$c_{F2}^{up} = (2\sqrt{\tilde{r}\tilde{D}} - v)$. Here, $r = f(0)$ and $\tilde{r} = \tilde{f}(0)$. As μ and σ increase, the propagation wave speeds approach the speed of the second Fisher approximation from above. The downstream propagation speed of the two-compartment system is bounded from above by the first Fisher's speed approximation and below by the second Fisher's speed approximation. The upstream propagation speed is bigger than both of the approximations but approaches the second Fisher approximation. That is, for smaller values of μ and σ, the population in (3) propagates downstream faster and is not washed away as fast as either of the Fisher's approximation would suggest. Fig. 9 shows the positive effect of the benthic component on the ability of the population to spread and resist being washed out.

7. Discussion

We presented a model of a population where individuals spend a proportion of their time immobile and a proportion of their time in an environment with a unidirectional current. Examples of such populations include marine species residing within coastal unidirectional currents, plants with windblown seeds, and aquatic insects in streams. In particular, we addressed 'the drift paradox' (Müller, 1954; Hershey et al., 1993) which poses the question of why there are aquatic insects in the upper reaches of streams if they are constantly subject to downstream drift.

Our results shed insight on three of the mechanisms for the resolution of the drift paradox identified in Section 1. First is Waters' hypothesis (Waters, 1972) that if individuals enter drift only when the population has reached a carrying capacity at the site, the population will persist. As stated, this hypothesis is trivial, as persistence is determined by the dynamics of a population at low densities, and the assumption is that there is no movement at low densities. We show that if the per capita local growth rate of a small population on the benthos, r, is higher than the per capita rate at which individuals enter the drift, μ, the population will always persist on the domain irrespective of the carrying capacity. This is intuitive: more individuals stay on the bottom of the stream than leave, and therefore the benthic population is never fully depleted. Waters' scenario is subsumed in this case.

If the rate of drift entry is faster than the local growth rate, we show that the population can still persist in a finite stream reach, given that the stream reach is sufficiently long and current speed is sufficiently low. This case addresses two other mechanisms counteracting downstream drift, variability in the direction of the current flow (e.g. turbulence) and individual swimming. We found the balance between the current speed vs. the stream heterogeneity and swimming necessary for population persistence in our system. In particular, Fig. 1 shows the critical domain size that guarantees persistence of a population in our model. The critical domain size is an increasing function of the stream current speed, v, and at a critical value v_L^* the critical domain size becomes infinite, and a population cannot persist on any finite stream reach. The model we analyzed extends the current theory of critical domain size in spatial models (Okubo et al., 2001, pp. 310–317) to include systems with persistent unidirectional flow. We also found the speeds at which a population spreads both up- and downstream (Figs. 5 and 6).

Our results show a strong connection between persistence criteria and propagation speeds. In particular, the current speed, v_L^*, at which the critical domain size is infinite is the same as the current speed, v_c^*, for which the population switches from spreading upstream to retreating. This connection between persistence and spread, while biologically reasonable, has been made precise in our paper through the use of model analysis. While we show this connection in the context of our particular model, we would conjecture that the same relationship, i.e. population spread stops when the critical domain size becomes infinite, holds in a wide range of systems.

While the model presented in this paper is a good starting point for analysis, some of the model assumptions are oversimple. For example, drift mortality (Allan, 1995, pp. 176–185), long-distance dispersal (Lutscher et al., 2004), and environmental heterogeneity are some of the important factors that we have not included. Representation of the flow in the model is also simple and can be extended to incorporate turbulence (Okubo, 1984) and depth-dependent velocity (Speirs and Gurney, 2001; Holmes, 2001). The model in this paper is a simplification of the more detailed model of stream communities that we are developing (Speirs et al., unpublished) where we focus on a stage-structured population of aquatic insects with the individuals in the larval stage residing in the stream and adults dispersing through air. Adult flight may play an important role for population persistence upstream (Hershey et al., 1993), and therefore, is an important component of the more detailed model. This model will allow us to determine the contribution of benthic crawling and adult upstream flight to population persistence. The more detailed model also includes some widely observed insect behavior such as dependence of the leaving rate from the benthos on resource availability and density of larvae (Hershey et al., 1993; Allan, 1995, pp. 51–59; Siler et al., 2001). However, the simplified model allowed us to mathematically develop the theory of persistence and spread of populations in systems with unidirectional flow and mobile and stationary subpopulations. Work presented in this paper is a step towards a better understanding of a balance of

factors and their combinations that resolve the drift paradox.

Acknowledgments

This work was greatly helped by discussions with Bill Gurney, Dougie Speirs and Steven Holmes, who generously shared unpublished results. We thank Kurt Anderson, Scott Cooper, and Sebastian Diehl for discussions of the stream communities dynamics, and Jason Sundram for help with coding. This work was supported by the US National Science Foundation (NSF DEB01-08450), University of Alberta, by an NSERC operating grant, and a Canada Research chair.

Appendix A

In this appendix, we derive the persistence condition for system (4). We first find the solution for n_d. To do this, we collapse system (4) into a single partial differential equation for n_d with an additional integral term. This equation is then solved using separation of variables.

Applying variation of constants formula to the second equation of (4) and write n_b in terms of n_d as

$$n_b(x,t) = e^{-(\mu-1)t}n_b(x,0) + \sigma e^{-(\mu-1)t}\int_0^t e^{(\mu-1)\tau}n_d(x,\tau)\,\mathrm{d}\tau. \tag{25}$$

Without loss of generality, we can assume that $n_b(x, 0)$ is 0. In other words, all individuals are initially in the mobile class n_d. While this may not reflect biologically realistic initial conditions, the addition of the exponentially decreasing term $e^{-(\mu-1)t}n_b(x,0)$ does not change the stability properties of the linear system. Plugging this expression for n_b into the first equation of (4) and setting $u = n_d e^{(\mu-1)t}$ and $\alpha = \sigma - \mu + 1$ we obtain

$$\frac{\partial u}{\partial t} = \frac{\partial^2 u}{\partial x^2} - v\frac{\partial u}{\partial x} - \alpha u + \mu\sigma\int_0^t u(\tau)\,\mathrm{d}\tau. \tag{26}$$

We now find the solution for $u(x, t)$ by separation of variables. Set $u = X(x)T(t)$. Then we need to solve the following two equations

$$T'(t) - \mu\sigma\int_0^t T(\tau)\,\mathrm{d}\tau + (\alpha+\lambda)T(t) = 0 \tag{27}$$

and

$$X''(x) - vX'(x) + \lambda X(x) = 0, \tag{28}$$

where λ is a constant.

The solution to (27) is

$$T(t) = c_1 m_1 e^{m_1 t} + c_2 m_2 e^{m_2 t}, \tag{29}$$

where

$$m_{1,2} = \frac{-(\alpha+\lambda) \pm \sqrt{(\alpha+\lambda)^2 + 4\mu\sigma}}{2}. \tag{30}$$

Note that $m_{1,2}$ are always real. Furthermore, m_1 is a decreasing function of $\lambda > 0$. This can be seen by differentiating m_1 with respect to λ.

We now turn to Eq. (29). The boundary conditions are

$$X'(0) - vX(0) = 0,$$
$$X(L) = 0. \tag{31}$$

The solution to (29) is given by

$$X(x) = a_1 e^{l_1 x} + a_2 e^{l_2 x}, \tag{32}$$

where

$$l_{1,2} = \frac{v \pm \sqrt{v^2 - 4\lambda}}{2}. \tag{33}$$

We now consider several cases for the value of λ. If $\lambda < 0$ then $l_{1,2}$ are real and positive. Applying the boundary conditions, we find that the only solution is the trivial solution. If $\lambda > 0$ then there are two possibilities. First, suppose that $v^2 \geqslant 4\lambda$. In this case, $l_{1,2}$ are still real and positive, and the solution is again trivial. Secondly, if $v^2 < 4\lambda$, then $l_{1,2}$ have non-trivial imaginary parts and the solution for $X(x)$ is given by

$$X(x) = a_3 e^{vx/2}\cos\left(x\sqrt{4\lambda - \frac{v^2}{2}}\right) + a_4 e^{vx/2}\sin\left(x\sqrt{4\lambda - \frac{v^2}{2}}/2\right). \tag{34}$$

Applying boundary conditions, we find that λ must satisfy

$$\frac{\sqrt{4\lambda - v^2}}{v} + \tan\left(\frac{\sqrt{4\lambda - v^2}}{2}L\right) = 0. \tag{35}$$

This equation has a series of solutions $\lambda_n(v, L)$ with $\lambda_1 < \lambda_2 < \ldots$. Corresponding to each λ_n we have $m_1(\lambda_n) = m_{1n}$ and $m_2(\lambda_n) = m_{2n}$.

Thus, we can now write the solution for $u(x, t)$ and therefore for $n_d(x, t)$:

$$n_d(x,t) = \sum_{n=1}^{\infty}\left[c_1 m_{1n} e^{(m_{1n}-(\mu-1)t)} + c_2 m_{2n} e^{(m_{2n}-(\mu-1))t}\right] \times\left[e^{vx/2}\left(a_3\cos\left(\frac{\sqrt{4\lambda_n - v^2}}{2}x\right) \times + a_4\sin\left(\frac{\sqrt{4\lambda_n - v^2}}{2}x\right)\right)\right]. \tag{36}$$

We see that $n_d \to 0$ as $t \to \infty$ if $(c_1 m_{1n} e^{(m_{1n}-(\mu-1))t} + c_2 m_{2n} e^{(m_{2n}-(\mu-1))t}) \to 0$. The expression in brackets converges to zero if the exponents are negative. Since

$m_{1n} > m_{2n}$, it suffices to require the first exponent to be negative. Therefore, if

$$m_{11} - (\mu - 1) = \left[\frac{-(\alpha + \lambda_1(v, L))^2 + \sqrt{(\alpha + \lambda_1(v, L)) + 4\mu\sigma}}{2} - (\mu - 1)\right] < 0 \tag{37}$$

then $n_d \to 0$ as $t \to \infty$, and the population goes extinct. This implies that for a population to persist, it is necessary that

$$\lambda_1(v, L) < \frac{\sigma}{\mu - 1}. \tag{38}$$

Appendix B

In this appendix, we derive the up- and downstream propagation speeds for (9). To do this we consider the characteristic polynomials P_0 and P_1 of the zero and the non-zero steady states, respectively. First, using Descarte's rule of sign, we determine the possible dimensions of the stable manifold of the zero and of the unstable manifold of the non-zero steady states. We then consider the characteristic polynomials P_0 and P_1 in more detail to determine the constraints on the values of the propagations speeds.

B.1. Case $\mu < 1$

Using Descarte's rule of signs we determine the number of real roots of P_0 and P_1. For both upstream and downstream facing waves these indicate that (1) the possible dimensions of the stable manifold of the zero steady state, D_0, are 0 or 2; and (2) the possible dimensions of the unstable manifold of the non-zero steady states, D_1, are 1 or 3. For a heteroclinic orbit to exist, both D_0 and D_1 must be positive. Since D_0 can be 0, we must consider the roots of P_0 in more detail.

We require P_0 to have at least one real negative root. Moreover, if the non-positive roots of P_0 had non-zero imaginary parts, then the approach to the steady state would be oscillatory. In that case, solutions would become negative, which is unrealistic. At the transition point between 0 and 2 real negative roots, P_0 looks as in Fig. 10, i.e. the graph of P_0 touches the axis. Mathematically, this corresponds to the conditions $P_0'(\lambda) = 0$ and $P_0(\lambda) = 0$ for some $\lambda < 0$.

Consider

$$P_0'(\lambda) = -3\lambda^2 + 2A_1\lambda + A_2 = 0. \tag{39}$$

The solutions to this equation are

$$\lambda_{1,2} = \frac{A_1 \pm \sqrt{A_1^2 + 3A_2}}{3}. \tag{40}$$

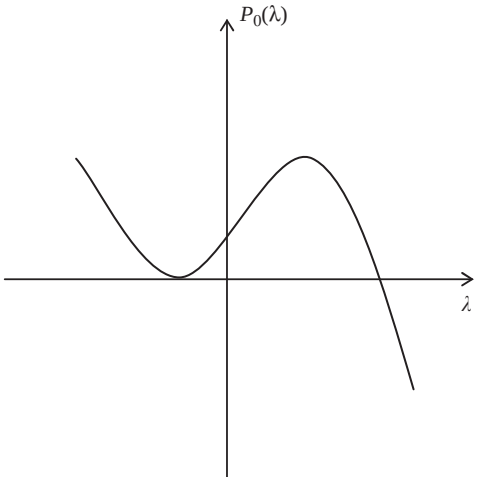

Fig. 10. The shape of $P_0(\lambda)$ when its two roots switch from complex to real.

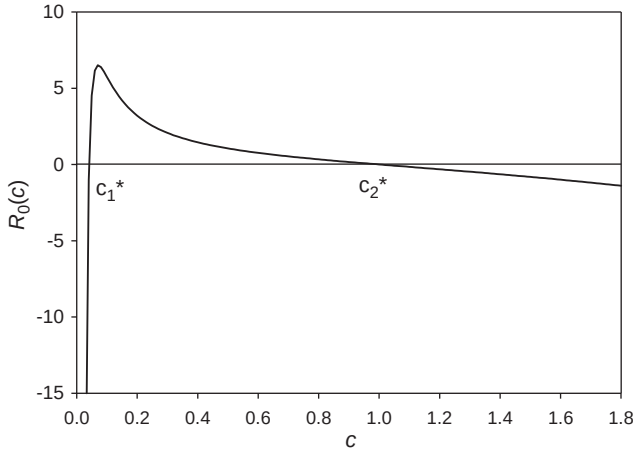

Fig. 11. $R_0(c)$ vs. the propagation speed c for $\mu = 0.8$ and $\sigma = 0.8$. If $R_0(c)$ is negative then the orbit is possible. $R_0(c)$ has two roots $c \approx 0.04$ and 1.05 which were found numerically.

Note that P_0' has one positive and one negative root. The positive root corresponds to the local maximum of P_0, and the negative root corresponds to the local minimum of P_0 (Fig. 10). P_0 touches the x-axis at λ_2 exactly if λ_2 is a root of P_0. Since the coefficients of P_0 are functions of c, we define

$$R_0(c) = P_0(\lambda_2) = -\lambda_2^3 + A_1\lambda_2^2 + A_2\lambda_2 + A_3. \tag{41}$$

If $R_0 > 0$, then P_0 has no real negative roots. If $R_0 < 0$, then P_0 has two real negative roots. The critical value is $R_0(c^*) = 0$, which gives a threshold value for the propagation speed. Fig. 11 shows a plot of $R_0(c)$ for $v = 0.0$, $\mu = 0.8$ and $\sigma = 0.8$. $R(c)$ has two positive roots $c_1^* \approx 0.04$ and $c_2^* \approx 1.05$, which were found numerically. Fig. 11 shows that $R_0(c) > 0$ for $c_1^* < c < c_2^*$ and hence, there is no traveling wave for these values of c. Using the

argument from Lewis and Schmitz (1996), we can show that if $v = 0$, the orbit spirals as it approaches (0,0,0) for $c \in (0, c_1^*]$, and n_b or n_d become negative. By continuity, the orbit remains spiral for small enough values of v. This argument allows us to exclude the range $c \in (0, c_1^*]$ as possible propagation speeds, at least for small v. Therefore, $c \in [c_2^*, \infty)$ is the range for the propagation speeds. Whether the same reasoning is true for large values of v remains an open question. The traveling speed c^* can also be interpreted as the rate at which a locally introduced population will spread into a new environment, providing the initial beachhead of individuals occupies a finite region. This connection between the traveling wave speed and the rate of spread of locally introduced individuals is proved in detail for the case $v = 0$ in Hadeler and Lewis (2004).

B.2. Case 2: $\mu \geqslant 1$

If the either downstream or upstream wave is spreading, then the dimensions D_0 and D_1 are as in the previous section ($\mu < 1$). Thus, we examine P_0 as before to find the possible range of values of the propagation speed. Now, however, there is only one root c_1^* of the corresponding polynomial $R_0(c)$.

We also must include the possibility that the wave is retreating. We find that in this case D_0 is always 1 for downstream facing waves. For upstream facing waves, if $\mu = 1$, the D_0 is 1 for all c; if $\mu > 1$, D_0 is 1 when $c > v$ (wave is retreating faster than advection speed), and either 1 or 3 if $c < v$ (wave is retreating slower than advection speed). D_1 can be either 0 or 2 in all cases. We first examine this case using biological reasoning, and then use numerical simulations to show that the biological argument is valid. In the absence of advection, the population propagates up- and downstream with positive speeds. Therefore, if we add advection, we do not expect the downstream wave to retreat. Nor do we expect the upstream wave to retreat faster than the advection, i.e. to have $c > v$. Numerical methods confirm this reasoning as follows. We know that in both of these cases P_0 has one real negative root. We numerically explored the corresponding eigenvectors for ranges of parameters $1 < \mu < 100$, $0 < \sigma < 100$, $-100 < v < 100$, and $-100 < c < 0$. The first and second component of the eigenvector, which correspond to n_b and n_d, have opposite sign. This means that either n_b or n_d are negative as the orbit approaches the zero steady state, which is unrealistic.

The only remaining case is $c < v$ (upstream facing wave is retreating slower than advection). Using the same argument as described in the previous paragraph, we found that an orbit is not possible when P_0 has only one negative real root. For $\mu = 1$ implies that an orbit is not possible in this case either. Thus, if $\mu = 1$, traveling waves are not possible with negative propagation speeds, and the population will always spread up and downstream. This observation is supported by our numerical simulations.

If $\mu > 1$, the desired heteroclinic orbit is possible if P_0 has three negative real roots. From here, we can continue as before. We set

$$R_0(c) = -\lambda_1^3 + A_1\lambda_1^2 + A_2\lambda_1 + A_3 = 0, \tag{42}$$

where λ_1 is the solution to $P_0'(\lambda) = 0$ in (40). This gives a single negative root that corresponds to the negative upstream propagation speed. Moreover, if P_0 has three negative real roots, then the non-zero steady state has a two-dimensional unstable manifold. To see that this is true, we find $R_1(c)$ for $P_1(\lambda)$ where

$$R_1(c) = -\lambda_2^3 + B_1\lambda_2^2 + B_2\lambda_2 + B_3 = 0, \tag{43}$$

where λ_2 is the larger root of $P_1'(\lambda) = 0$. The range of c for which the zero steady state has three real negative eigenvalues is within the range of c for which the non-zero steady state has two positive eigenvalues.

References

Alexander, S.E., Roughgarden, J., 1996. Larval transport and population dynamics of intertidal barnacles: a coupled benthic/oceanic model. Ecol. Monogr. 66, 259–275.

Allan, J.D., 1995. Stream Ecology: Structure and Function of Running Waters. Chapman & Hall, London.

Anholt, B.R., 1995. Density dependence resolves the stream drift paradox. Ecology 76, 2235–2239.

Ballyk, M., Smith, H., 1999. A model of microbial growth in a plug flow reactor with wall attachment. Math. Biosci. 158, 95–126.

Ballyk, M., Dung, L., Jones, D.A., Smith, H.L., 1998. Effects of random motility on microbial growth and competition in a flow reactor. SIAM J. Appl. Math. 59, 573–596.

Bird, G.A., Hynes, H.B.N., 1981. Movements of adult insects near streams in southern Ontario. Hydrobiologia 77, 65–69.

Elliot, J.M., 1971. Upstream movements of benthic invertebrates in a Lake District stream. J. Anim. Ecol. 40, 235–252.

Gaines, S.D., Bertness, M.D., 1992. Dispersal of juveniles and variable recruitment in sessile marine species. Nature 360, 579–580.

Gaylord, B., Gaines, S.D., 2000. Temperature or transport? Range limits in marine species mediated solely by flow. Am. Nat. 155, 769–789.

Hadeler, K.P., Lewis, M.A., 2004. Spatial dynamics of the diffusive logistic equation with sedentary compartment. Can. Appl. Math. Quart. 10, 473–500.

Hershey, A.E., Pastor, J., Peterson, B.J., Kling, G.W., 1993. Stable isotopes resolve the drift paradox for *Baetis* mayflies in an arctic river. Ecology 74, 2315–2325.

Holmes, S., 2001. Turbulent flows and simple behaviours. Their effect on strategic determination of population persistence. Ph.D. Thesis, University of Strathclyde, Glasgow.

Humphries, S., Ruxton, G.D., 2002. Is there really a drift paradox? J. Anim. Ecol. 71, 151–154.

Lancaster, J., 2000. Geometric scaling of microhabitat patches and their efficacy as refugia during disturbance. J. Anim. Ecol. 63, 442–457.

Lancaster, J., Hildrew, A.G., 1993a. Characterising instream flow refugia. Can. J. Fish. Aquat. Sci. 50, 1663–1675.

Lancaster, J., Hildrew, A.G., 1993b. Flow refugia and the microdistribution of lotic macroinvertebrates. JNABS 12, 285–393.

Lewis, M.A., Kareiva, P., 1993. Allee dynamics and the spread of invading organisms. Theor. Popul. Biol. 43, 141–158.

Lewis, M.A., Schmitz, G., 1996. Biological invasion of an organism with separate mobile and stationary states: modeling and analysis. Forma 11, 1–25.

Lewis, M.A., Schmitz, G., Kareiva, P., Trevors, J.T., 1996. Models to examine containment and spread of genetically engineered microbes. Mol. Ecol. 5, 165–175.

Lutscher, F., Pachepsky, E., Lewis, M.A., 2004. The effect of dispersal patterns on stream populations. SIAM Applied Math., in press.

Müller, K., 1954. Investigations on the organic drift in North Swedish streams. Report of the Institute of Freshwater Research, Drottningholm, vol. 34, pp. 133–148.

Müller, K., 1982. The colonization cycle of freshwater insects. Oecologia 53, 202–207.

Murray, J.D., 1989. Mathematical Biology. Springer, Berlin.

Okubo, A., 1984. Oceanic turbulent diffusion of abiotic and biotic species. Mathematical Ecology, Lecture Notes in Biomathematics, vol. 54. Springer, Berlin.

Poff, N.L., Ward, J.V., 1992. Heterogeneous currents and algal resources mediate in situ foraging activity of a mobile stream grazer. Oikos 65, 465–487.

Rempel, L.L., Richardson, J.S., Healey, M.C., 1999. Flow refugia for benthic marcoinvertebrates during flooding of a large river. JNABS 18, 24–48.

Siler, E.R., Wallace, J.B., Eggert, S.L., 2001. Long-term effects of resource limitation on stream invertebrate drift. Can. J. Fish Aquat. Sci. 58, 1624–1637.

Speirs, D.C., Gurney, W.S.C., 2001. Population persistence in rivers and estuaries. Ecology 82, 1219–1237.

Strauss, W.A., 1992. Partial Differential Equations: An Introduction. Wiley, New York.

Waters, R.F., 1972. The drift of stream insects. Annu. Rev. Entomol. 17, 253–272.

Williams, D.D., Williams, N.E., 1993. The upstream/downstream movement paradox of lotic invertebrates: quantitative evidence from a Welsh mountain stream. Freshwater Biol. 30, 199–218.

Winterbourn, M.J., Crowe, A.L.M., 2001. Flight activity of insects along a mountain stream: is directional flight adaptive? Freshwater Biol. 46, 1479–1489.

Winterbottom, J.H., Orton, S.E., Hildrew, A.G., 1997a. Field experiments on the mobility of benthic invertebrates in a southern English stream. Freshwater Biol. 38, 37–47.

Winterbottom, J.H., Orton, S.E., Hidrew, A.G., Lancaster, J., 1997b. Field experiments on flow refugia in streams. Freshwater Biol. 37, 569–580.